HIGH ORDER SENSITIVITY ANALYSIS OF A MISTUNED BLISK INCLUDING INTENTIONAL MISTUNING

Linus Pohle, Sebastian Tatzko, Lars Panning-von Scheidt, Jörg Wallaschek

Leibniz Universität Hannover, Institute of Dynamics and Vibration Research, Hannover, Germany

e-mail: linuspohle@gmx.de

Small deviations between turbine blades exist due to manufacturing tolerances or material inhomogeneities. This effect is called mistuning and usually causes increased vibration amplitudes and also a lower service life expectancy of bladed disks or so called blisks (bladed integrated disk). The major resulting problem is to estimate the maximum amplitude with respect to these deviations. Due to the probability distribution of these deviations, statistical methods are used to predict the maximum amplitude. State of the art is the Monte-Carlo simulation which is based on a high number of randomly re-arranged input parameters. The aim of this paper is to introduce a useful method to calculate the probability distribution of the maximum amplitude of a mistuned blisk with respect to the random input parameters. First, the applied reduction method is presented to initiate the sensitivity analysis. This reduction method enables the calculation of the frequency response function (FRF) of a Finite Element Model (FEM) in a reasonable calculation time. Based on the Taylor series approximation, the sensitivity of the vibration amplitude depending on normally distributed input parameters is calculated and therewith, it is possible to estimate the maximum amplitude. Calculating only a single frequency response function shows a good agreement with the results of over 1000 Monte-Carlo simulations.

Keywords: turbine blades, mistuning, sensitivity analysis

Nomenclature

d_0	–	structural damping	σ	–	standard deviation
k	–	blade index	$\mathbf{I}$	–	identity matrix
u	–	modal displacement	$\mathbf{K}_b$	–	stiffness matrix of blades
x	–	geometric displacement	$\mathbf{K}_d$	–	stiffness matrix of one disk segment
EO	–	engine order	$\mathbf{K}_b^{\mathrm{A}}$	–	stiffness matrix of blades, type A
N	–	number of blades	$\widetilde{[\cdot]}$	–	reduced system matrices
δ_k	–	mistuning factors	$\widehat{[\cdot]}$	–	absolute amplitude
α	–	tolerance interval	$[\cdot]^{\mathrm{H}}$	–	Hermitian transpose

1. Introduction

A blade integrated disk (blisk), i.e. blades and disk made out of one piece, has a lot of technical benefits like weight reduction or omission of fretting between the blade and disk. This causes lower damping and higher structural coupling between the blades. Due to small deviations between the blade properties, energy localization can occur causing considerably higher vibration amplitudes of a few blades. Whitehead (1966) gave a limit for the maximum vibration amplitude of a mistuned blisk. This theoretical maximum is existent, if all modes have the same eigenfrequency and are in phase at one blade position.

The dynamical behavior of one blade mode can be simulated with a cyclic lumped-mass model (see e.g. Griffin and Hoosac, 1984). The benefits of such a simple model is the simple dynamical behavior and the low calculation time. However, different mode families and multiple mode shapes cannot be described by this model. On the other hand, high computational cost is inevitable to solve a full Finite Element model of a mistuned blisk. Especially for parameter studies, a high number of high-resolution FRF's is necessary. Therefore, a lot of different reduction methods are developed to calculate the FRF of a mistuned blisk with a lower computational effort.

There are two ways that are frequently used to reduce the number of DOF of a mistuned blisk. On the one hand, the model can be described by the system modes (called Subset of Nominal Modes, SNM), which is described in Yang and Griffin (2001), extended to geometric mistuning in Sinha (2009) and compared to the first version of the SNM in Bhartiya and Sinha (2011). The model of the whole blisk is divided into single sectors which could be reduced by a modal transformation using the modes of the segment. Afterwards, the mistuned stiffness matrix can be calculated very efficiently, and a good agreement to the full model can be shown. If there is only one mode describing the blade dominant vibration, this method can be extended to the Fundamental Model of Mistuning (FMM), which was introduced in Feiner and Griffin (2002). The main condition is that the mode shape remains almost unchanged and only small difference occurs between the blades eigenfrequencies. The main benefit is that the knowledge of the system matrices of the Finite Element model is not required. This method is very useful for the identification of mistunig, see Shuai and Jianyao (2010), Feiner and Griffin (2004a,b).

On the other hand, one sector can be divided into a blade and a disk sector. After modal reduction of these components, the matrices are coupled and the dynamical behavior of the whole mistuned blisk can be calculated. This so-called Component Mode Synthesis (see e.g. Bladh *et al.*, 2001a,b) needs more computational effort to regard mistuning, but is much more flexible (see Moyroud *et al.* (2002), for comparison, Castanier and Pierre (2006) for an overview). It is assumed that the disk is cyclic symmetric. Thus it can be described by cyclic boundary conditions (see Thomas (1979) for a description). The DOFs of the blade are reduced by the well-known Craig Bampton method (see Craig and Bampton, 1968; Craig, 2000). This method was extended in Hohl *et al.* (2011) using a reduction of the coupling nodes using Wave-Based Substructuring Čermelj *et al.* (2008) and a secondary modal reduction.

To analyze the influence of mistuning, Monte-Carlo Simulation (MCS) can be used to find an optimal pattern or to find the maximum amplitude of a given probability distribution of the eigenfrequencies, see Hohl *et al.* (2011). In Bladh *et al.* (2001), it is shown that only 50 MCS are necessary to fit the probability density function (PDF) of the maximum vibration amplitude over all frequencies. The PDF is fitted with a Weibull distribution. In Mignolet and Hu (1997), a direct prediction method describes how to find the maximum amplitude for one frequency using the cumulates of the normal distributions. The distribution of a lumped-mass model with one DOF per segment results in a Gaussian distribution.

The presented paper introduces a new method to find the Gaussian distribution of a mistuned blisk. The aim of the paper is to show the benefits of these methods and its possible application. First, the used reduction method is described and the universal validity is given. Thereafter, high order sensitivity analysis is shown and compared to the MCS. The second case study emphasizes its versatile application spectrum based on an intentional mistuned example. Therewith, the dynamical behavior of a mistuned blisk can be analyzed depending on different mistuning factors, engine order, or blade pattern.

2. Reduction method

The first example analyzed is a simplified blisk with $N = 12$ blades (see picture in Fig. 1). This blisk exhibits the typical dynamical behavior of a blisk without spinning effects like spin softening, centrifugal stiffening or Coriolis effects. The blisk is cyclic symmetric with 12 blades ignoring manufacturing tolerances. Thus, cyclic symmetry can be used to analyze the full blisk regarding only one sector.

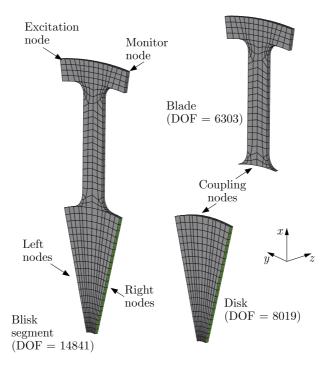Fig. 1. Picture of the analyzed blisk

Fig. 2. Finite Element mesh with special nodes of interest

In Fig. 2, the mesh of such a sector is shown. The mesh of the whole system has about 170 000 degrees of freedom (DOF) and a harmonic analysis of the vibration amplitudes cannot

be solved at a common PC in a reasonable time, especially if parameter variations are processed or optimization problems are considered. Regarding cyclic symmetry, the number of DOFs is reduced to 14841 for the calculation. The excitation node and the monitor node are located at the blade tip, and the direction of excitation and monitoring is the z-direction. Of course, the following shown method can be used to analyze a blisk with any arbitrary geometry.

In Fig. 3, the nodal diameter diagram is illustrated for the first four mode families. The first mode family is well separated, and will be used for the analysis in this paper. Nevertheless, the results are verified for other mode families as well. Some chosen mode shapes of the tuned system are depicted in Fig. 3.
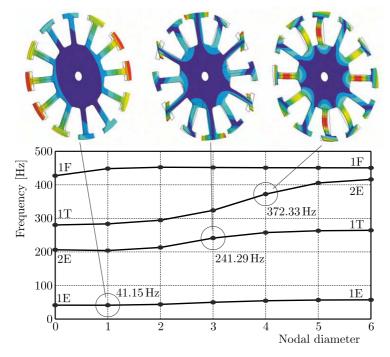

Fig. 3. Nodal diameter diagram

In general, the equation of the dynamical system can be written as

$$\mathbf{M}\ddot{\mathbf{x}}(t) + \mathbf{D}\dot{\mathbf{x}}(t) + \mathbf{K}\mathbf{x}(t) = \mathbf{F}(t) \tag{2.1}$$

with $\mathbf{M}$, $\mathbf{D}$, and $\mathbf{K}$ as the mass, damping, and stiffness matrix. The excitation force vector $\mathbf{F}(t)$ is assumed to be harmonic in time with a constant phase shift between the blades depending on the engine order EO

$$\mathbf{F}(t) = \widehat{\mathbf{F}}\mathrm{e}^{\mathrm{i}\Omega t} = \begin{bmatrix} 1 \\ \vdots \\ \mathrm{e}^{-\mathrm{i}k\phi} \\ \vdots \\ \mathrm{e}^{-\mathrm{i}(N-1)\phi} \end{bmatrix} \widehat{f}\mathrm{e}^{\mathrm{i}\Omega t} \tag{2.2}$$

with the phase shift

$$\phi = \frac{2\pi EO}{N} = \text{ const} \tag{2.3}$$

The damping is modeled as structural damping depending on the stiffness matrix

$$\mathbf{D} = \frac{d_0}{\Omega}\mathbf{K} \tag{2.4}$$

Using the modal transformation into the frequency domain with the harmonic approach $\mathbf{x}(t) = \widehat{\mathbf{x}} \exp(\mathrm{i}\Omega t)$, Eq. (2.1) reads

$$\widehat{\mathbf{x}}(\Omega) = [-\mathbf{M}\Omega^2 + (1 + \mathrm{i}d_0)\mathbf{K}]^{-1}\widehat{\mathbf{F}} \tag{2.5}$$

The attentive reader notices that the equation of motion is build up for a linear model. The following process will be described for such a model. Nevertheless, it will be very simple to include rotating effects like centrifugal or Coriolis forces. Therefore, the matrices have to be checked for nonsymmetry and varity over the rotation speed. The following reduction method is limited to linear models, but other reduction methods for nonlinear models can be used.

For a large number of DOFs a lot of computational effort is required to calculate the combined matrix $(-\mathbf{M}\Omega^2 + (1 + \mathrm{i}d_0)\mathbf{K})^{-1}$.

The chosen reduction method is based on the Component Mode Synthesis (CMS) extended by the Wave-Based Substructuring (WBS) (see Hohl *et al.*, 2011). Firstly, the structural matrices are divided into master nodes (m) and slave nodes (s) as described in Craig and Bampton (1968). The master nodes are the coupling nodes between the blades and the disk (see Fig. 2). The slave nodes are transformed to a small basis of mode shapes. Therefore, the reduced stiffness matrix $\widetilde{\mathbf{K}}_b$ of one blade b is obtained by

$$\widetilde{\mathbf{K}}_b = \begin{bmatrix} \mathbf{K}_{mm} & \widetilde{\mathbf{K}}_{ms} \\ \widetilde{\mathbf{K}}_{sm} & \widetilde{\mathbf{K}}_{ss} \end{bmatrix} = \begin{bmatrix} \mathbf{I} & \mathbf{0} \\ \boldsymbol{\Psi} & \boldsymbol{\Phi} \end{bmatrix}^{\mathrm{H}} \begin{bmatrix} \mathbf{K}_{mm} & \mathbf{K}_{ms} \\ \mathbf{K}_{sm} & \mathbf{K}_{ss} \end{bmatrix} \begin{bmatrix} \mathbf{I} & \mathbf{0} \\ \boldsymbol{\Psi} & \boldsymbol{\Phi} \end{bmatrix} \tag{2.6}$$

where $\mathbf{I}$ is the identity matrix, $(\cdot)^{\mathrm{H}}$ denotes the Hermitian transformation and

$$\boldsymbol{\Psi} = -\mathbf{K}_{ss}^{-1}\mathbf{K}_{sm} \tag{2.7}$$

and $\boldsymbol{\Phi}$ is the modal matrix which contains the eigenvectors of the generalized eigenvalue problem

$$\mathbf{K}_{ss}\boldsymbol{\Phi} = \mathbf{M}_{ss}\boldsymbol{\Phi}\lambda \tag{2.8}$$

Accordingly, the mass matrix is subdivided and reduced. The disk can be reduced using a cyclic symmetric model as shown in Thomas (1979). Thus, all tuned sectors have the same dynamic properties. To couple the segments, it is assumed that the nodes on the right hand side $\mathbf{u}_{k,\mathrm{R}}$ have the same motion as the nodes on the left hand side $\mathbf{u}_{k,\mathrm{L}}$, except for the phase shift (see Fig. 2). Hence, the displacement of the nodes can be rewritten in cyclic coordinates by

$$\mathbf{u}_k = \begin{bmatrix} \mathbf{u}_{k,\mathrm{L}} \\ \mathbf{u}_{k,\mathrm{M}} \\ \mathbf{u}_{k,\mathrm{R}} \end{bmatrix} = \begin{bmatrix} \mathbf{0} & \exp\!\left(-\mathrm{i}\frac{2\pi k}{N}\right) \\ \mathbf{I} & \mathbf{0} \\ \mathbf{0} & \mathbf{I} \end{bmatrix} \begin{bmatrix} \mathbf{u}_{k,\mathrm{M}} \\ \mathbf{u}_{k,\mathrm{R}} \end{bmatrix} \tag{2.9}$$

for each nodal diameter k. Due to this transformation, the mass matrix and the stiffness matrix can be formulated for each segment. After the Craig Bampton reduction of all blades, see Eq. (2.6), the reduced matrices can be written in the matrix of the full disk by using a subset of modes and the master nodes

$$\widetilde{\mathbf{K}}_d = \begin{bmatrix} \widetilde{\mathbf{K}}_{mm}[\operatorname{diag}(\widetilde{\mathbf{K}}_{d,ms})] \\ [\operatorname{diag}(\widetilde{\mathbf{K}}_{d,sm})] & [\operatorname{diag}(\widetilde{\mathbf{K}}_{d,ss})] \end{bmatrix} \tag{2.10}$$

with

$$[\operatorname{diag}(\widetilde{\mathbf{K}}_{d,ss})] = \begin{bmatrix} \widetilde{\mathbf{K}}_{d,ss,1} & \cdots & \mathbf{0} \\ \vdots & \ddots & \vdots \\ \mathbf{0} & \cdots & \widetilde{\mathbf{K}}_{d,ss,N} \end{bmatrix} \tag{2.11}$$

and just for $[\operatorname{diag}(\widetilde{\mathbf{K}}_{d,sm})]$ and $[\operatorname{diag}(\widetilde{\mathbf{K}}_{d,ms})]$. The coupling nodes have to be transformed into the full system using the theory of cyclic systems

$$\widetilde{\mathbf{K}}_{mm} = \begin{bmatrix} \widetilde{\mathbf{K}}_{1,1} & \widetilde{\mathbf{K}}_{1,2} & \cdots \\ \widetilde{\mathbf{K}}_{2,1} & \widetilde{\mathbf{K}}_{2,2} & \cdots \\ \vdots & \vdots & \ddots \end{bmatrix} \tag{2.12}$$

with the submatrices

$$\widetilde{\mathbf{K}}_{i,j} = \sum_{h=1}^{N-1} (w^{h(i-1)})^{\mathrm{H}} \widetilde{\mathbf{K}}_h w^{h(j-1)} \tag{2.13}$$

where

$$w = \mathrm{e}^{-\mathrm{i}\frac{2\pi}{N}} \tag{2.14}$$

As a consequence, the size of the structural matrices of the disk is strongly decreased. Nevertheless, the master nodes are in physical notation and can include a lot of DOFs. These coupling nodes are reduced by the single-value decomposition (SVD) of the modal matrix of the whole segment including the disk and the blade

$$\mathbf{K}_{\mathrm{seg}}\boldsymbol{\Phi}_{\mathrm{seg}} = \mathbf{M}_{\mathrm{seg}}\boldsymbol{\Phi}_{\mathrm{seg}}\lambda \tag{2.15}$$

The SVD of a subset of the modal matrix $\boldsymbol{\Phi}_{\mathrm{sub}} = \boldsymbol{\Phi}_{\mathrm{seg}}(\mathrm{cpl},\cdot)$, including only the coupling DOF, is given by

$$\boldsymbol{\Phi}_{\mathrm{sub}} = \mathbf{U}\boldsymbol{\Sigma}\mathbf{V}^{\mathrm{T}} \tag{2.16}$$

where $\boldsymbol{\Sigma}$ is a square diagonal matrix with non-negative real numbers on the diagonal. Using the matrix $\mathbf{U}$ to reduce the system with $\mathbf{U}_{\mathrm{red}} = \mathbf{U}(w,\cdot)$, the behavior of the coupled nodes can be projected in an accurate way. w is the number of waves chosen to describe the motion of the coupling nodes. The reduction method is called Wave-Based Substructuring (WBS) which is described in Čermelj $et\ al.$ (2008). In this way, the system matrices for the blades and the disk can be written as

$$\begin{bmatrix} \widetilde{\mathbf{K}}_{mm} & \widetilde{\mathbf{K}}_{ms} \\ \widetilde{\mathbf{K}}_{sm} & \widetilde{\mathbf{K}}_{ss} \end{bmatrix} = \overbrace{\begin{bmatrix} \mathbf{I} & \mathbf{0} \\ \boldsymbol{\Psi} & \boldsymbol{\Phi} \end{bmatrix}^{\mathrm{H}}}^{\mathrm{CMS}} \overbrace{\begin{bmatrix} \mathbf{U}_{\mathrm{red}} & \mathbf{0} \\ \mathbf{0} & \mathbf{I} \end{bmatrix}^{\mathrm{H}}}^{\mathrm{WBS}} \begin{bmatrix} \mathbf{K}_{mm} & \mathbf{K}_{ms} \\ \mathbf{K}_{sm} & \mathbf{K}_{ss} \end{bmatrix} \begin{bmatrix} \mathbf{U}^* & \mathbf{0} \\ \mathbf{0} & \mathbf{I} \end{bmatrix} \begin{bmatrix} \mathbf{I} & \mathbf{0} \\ \boldsymbol{\Psi} & \boldsymbol{\Phi} \end{bmatrix} \tag{2.17}$$

Thus, the physical DOF are described by

$$\begin{bmatrix} \mathbf{u}_m \\ \mathbf{u}_s \end{bmatrix} = \begin{bmatrix} \mathbf{U}^* & \mathbf{0} \\ \mathbf{0} & \mathbf{I} \end{bmatrix} \begin{bmatrix} \mathbf{I} & \mathbf{0} \\ \boldsymbol{\Psi} & \boldsymbol{\Phi} \end{bmatrix} \begin{bmatrix} \mathbf{x}_m \\ \mathbf{x}_s \end{bmatrix} \tag{2.18}$$

with a significantly smaller number of DOFs than the Finite Element model. After the assembly of the blades and the disks, the system matrices are reduced by the second modal reduction. This reduction is a good possibility to decouple the equation of motion, too. Therewith, equation of motion (2.5) can be written as a scalar function

$$u_i = \frac{\widetilde{\widetilde{F}}_i}{-\widetilde{\mathbf{M}}_{i,i}\Omega^2 + (1 + \mathrm{i}d_0)\widetilde{\mathbf{K}}_{i,i}} \tag{2.19}$$

One possibility to take into account the mistuning is to detune the single blades by a factor of

$$\mathbf{K}_{b,k} = \delta_k \mathbf{K}_{b,0} \Rightarrow \widetilde{\mathbf{K}}_{b,k} = \delta_i \widetilde{\mathbf{K}}_{b,0} \tag{2.20}$$

This can be a variation of Young's modulus. These factors are randomly built up by a standard deviation σ_0 and a mean value of 1. Afterwards, the full system can be reassembled using the subsystems

$$\widetilde{\mathbf{K}}_{sys} = \begin{bmatrix} [\operatorname{diag}(\widetilde{\mathbf{K}}_{b,ss})] & [\operatorname{diag}(\widetilde{\mathbf{K}}_{b,ms}] & \mathbf{0} \\ [\operatorname{diag}(\widetilde{\mathbf{K}}_{b,sm})] & \widetilde{\mathbf{K}}_{mm} & \widetilde{\mathbf{K}}_{d,ms} \\ \mathbf{0} & \widetilde{\mathbf{K}}_{d,sm} & \widetilde{\mathbf{K}}_{d,ss} \end{bmatrix} \tag{2.21}$$

where

$$[\operatorname{diag}(\widetilde{\mathbf{K}}_{b,ss})] = \begin{bmatrix} \delta_1\widetilde{\mathbf{K}}_{b,ss} & \cdots & \mathbf{0} \\ \vdots & \ddots & \vdots \\ \mathbf{0} & \cdots & \delta_N\widetilde{\mathbf{K}}_{b,ss} \end{bmatrix} \tag{2.22}$$

as the reduced diagonal matrix of all slave nodes of the mistuned blades. $\widetilde{\mathbf{K}}_{mm}$ is the diagonal matrix of the reduced coupling nodes and $\widetilde{\mathbf{K}}_{d,ss}$ is the reduced matrix of the blisk. The mass matrix is assembled in the same way. With the second modal reduction, the system is reduced to a very small number of DOFs and the equations are decoupled.

In Figs. 4a and 4b, a comparison between the reduced order model (ROM) and the FEM is given. The ROM is reduced from overall 170 000 DOF to 84 DOF for the whole system considering mistuning. To prove the capability of the reduced order model as an example a strongly mistuned blisk is used. Young's modulus of one blade is 20% higher than all other. To calculate 131 frequency points, the time needed for the FEM is about 5 minutes on a standard personal computer with a comercial Finite Element code. The calculated points are concentrated around the eigenfrequency to guaranty the absolute amplitude. The calculation of the FRF of the ROM (Eq. (2.19)) with 2000 frequency points requires only 5 seconds with a very good accuracy.
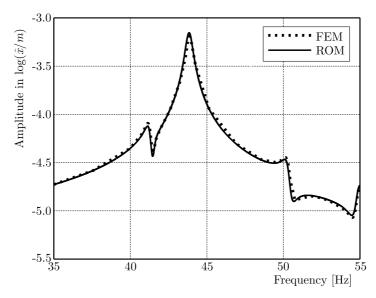

Fig. 4. Comparison between ROM and FEM: frequency response function of (a) 7th blade, (b) 9th blade

3. High order sensitivity analysis

One of the main points of interest is to calculate the maximum amplitude with respect to the standard deviation of the mistuned blades. In this way, the maximum stress can be determined.

Whitehead (1966) described the theoretical possible maximum of the amplitude of a mistuned blisk by

$$\frac{A_{max}}{A_{tuned}} = \frac{1}{2}(1 + \sqrt{N}) \tag{3.1}$$

with N denoting the number of blades. Here it is assumed that all vibration energy of all mode shapes is concentrated in one blade only. However, this case seems to be unreasonable for real bladed disk geometries. The common way to analyze the maximum amplitude of a mistuned bladed disk is the use of Monte-Carlo simulation (see Petrov, 2011; Siewert and Stüer, 2010; Beck *et al.*, 2012). The disadvantages are the very high calculation time and furthermore the lack of reliability of the results, e.g. there is no statement how many MCS are necessary to have convincing results. Using a Weibull estimation, the number of necessary MCS can be defined. Nevertheless, a high number of simulations is needed to obtain a good agreement (50 MCS in Bladh *et al.* (2001) and 500 MCS in Castanier and Pierre (2002)). Due to these problems, another method to calculate the maximum amplitude is given by a sensitivity analysis. This approach is motivated by Sextro *et al.* (2002), who described an extension of the theory of Sinha (1986) and Sinha and Chen (1989). To calculate the maximum amplitude with a given standard deviation of the stiffness of the blades, the sensitivity of the frequency response function is developed. By this means, an estimation of the maximum amplitude is very efficient and a statement of the probability of the amplitudes is given. The amplitude of the single blades can be written as

$$x = x_0 \pm \alpha\sigma \tag{3.2}$$

where x_0 is the average of all blades. Using the reduced DOF u in place of x economizes a lot of calculating time. It should be pointed out again that the equations of motion are decoupled and could be solved using scalar functions. This means that for calculation of the maximum and minimum limit of the tolerance interval of the amplitude, Eq. (3.2) can be written as

$$u = u_0 \pm \alpha\sigma \tag{3.3}$$

considering the transformation finally. Based on the results of Mignolet *et al.* (1999), it is assumed that the maximum amplitudes over all blades distributions at one frequency follow a Gaussian distribution. σ is the standard deviation and α the tolerance interval. $\alpha = 2$ means that 95.45% of all blade amplitudes are within the tolerance interval; for $\alpha = 3$, 99.73% of all blade amplitudes are within the interval. The definition given in Eq. (3.2) specifies the upper and lower limit for a given interval of the vibration amplitudes. In the case of N discrete data points, the standard deviation σ is defined as

$$\sigma = \sqrt{\frac{1}{N-1}\sum_{k=1}^{N}(u_k - u_0)^2} \tag{3.4}$$

Here, the amplitude of the single blades are used to calculate the standard deviation. It is assumed that the average amplitude of the vibration u_0 is the amplitude of the nominal, tuned system. The amplitude of the blade k is denoted as u_k. The parameters of interest are the mistuning factors δ_k introduced in the previous Section. The function of the amplitude depending on the variation factors can be approximated by a Taylor series

$$u_k(\delta_k) = u_0 + \sum_{h=1}^{\infty}\frac{1}{h!}\left(\frac{\partial u(\delta_k)}{\partial \delta_k}\right)^h\bigg|_{\delta_k=1}(\delta_k - 1)^h \tag{3.5}$$

The derivation of the equation of motion in Eq. (2.5) with respect to the mistuning factors reads

$$\frac{\partial u_i(\delta_k)}{\partial \delta_k} = \frac{-(1 + d_0\mathrm{i})\left(\frac{\partial \widetilde{K}_i}{\partial \delta_k}\right)\widetilde{\overline{F}}_i}{[-\widetilde{M}_i\Omega^2 + (1 + d_0\mathrm{i})\widetilde{K}_i(\delta_k)]^2} \tag{3.6}$$

where only the stiffness matrix depends on the mistuning factors. $\widetilde{K}_i$ denotes the scalar entry $\widetilde{\mathbf{K}}_{i,i}$ and $\widetilde{M}_i$ the scalar $\widetilde{\mathbf{M}}_{i,i}$. To calculate the higher terms of the Taylor series, the deviation with the higher order is

$$\frac{\partial^h u_i(\delta_k)}{\partial \delta_k^h} = \pm h! \left(\underbrace{\frac{(1 + d_0 \mathrm{i})\left(\frac{\partial \widetilde{K}_i}{\partial \delta_k}\right)}{[-\widetilde{M}_i \Omega^2 + (1 + d_0 \mathrm{i})\widetilde{K}_i(\delta_k)]}}_{=S} \right)^h u_i(\delta_k) \tag{3.7}$$

with "+" for even h and "−" for uneven h. Using the ratio test, it can easily be shown that the Taylor series converges if the supremum of S is less than 1. For this blisk, the maximum is $\delta_k = 10^{-3}$ like the maximum standard deviations of the single blades. As a consequence, the variance of the amplitude results in

$$\sigma_i = \sqrt{\frac{1}{N-1} \sum_{i=1}^{N} \left(\sum_{h=0}^{\infty} \pm (S)^h u_i(\delta_k) \right)^2} \tag{3.8}$$

In this equation, all variances are known from the system given in Eq. (2.5), except for the deviation of the stiffness matrix from Eq. (2.21) with respect to the mistuning factors

$$\frac{\partial \widetilde{\mathbf{K}}}{\partial \delta_k} = \begin{bmatrix} \left[\mathrm{diag}\left(\frac{\partial \widetilde{\mathbf{K}}_{b,ss}}{\partial \delta_k}\right) \right] & \mathbf{0} & \mathbf{0} \\ \mathbf{0} & \mathbf{0} & \mathbf{0} \\ \mathbf{0} & \mathbf{0} & \mathbf{0} \end{bmatrix} \tag{3.9}$$

with

$$\left[\mathrm{diag}\left(\frac{\partial \widetilde{\mathbf{K}}_{b,ss}}{\partial \delta_1}\right) \right] = \begin{bmatrix} \widetilde{\mathbf{K}}_{b,ss} & & \mathbf{0} \\ & \ddots & \\ \mathbf{0} & & \mathbf{0} \end{bmatrix} \tag{3.10}$$

followed by

$$\left[\mathrm{diag}\left(\mathrm{diag}\, \frac{\partial \widetilde{\mathbf{K}}_{b,ss}}{\partial \delta_2}\right) \right] = \begin{bmatrix} \mathbf{0} & & & \mathbf{0} \\ & \widetilde{\mathbf{K}}_{b,ss} & & \\ & & \ddots & \\ \mathbf{0} & & & \mathbf{0} \end{bmatrix} \tag{3.11}$$

and so on, until the last one

$$\left[\mathrm{diag}\left(\frac{\partial \widetilde{\mathbf{K}}_{b,ss}}{\partial \delta_N}\right) \right] = \begin{bmatrix} \mathbf{0} & & \mathbf{0} \\ & \ddots & \\ \mathbf{0} & & \widetilde{\mathbf{K}}_{b,ss} \end{bmatrix} \tag{3.12}$$

In Figs. 5a and 5b, the frequency response function is shown for a random mistuning pattern. The variance of the single blades is 10^{-3}, and three terms of the Taylor series are used. In Fig. 5a, the first isolated mode family is shown. Obviously, the FRFs of all blades are between the upper and the lower limit. The tolerance interval is set to $\alpha = 2$, therefore, the amplitude can be higher by 4.55% of the cases. Due to the upper limit, the deviation of the maximum amplitude is given for every frequency with the probability which is needed. In Fig. 5b, the region of nearby eigenfrequencies is shown. The limits show a good agreement with the randomly mistuned blades.
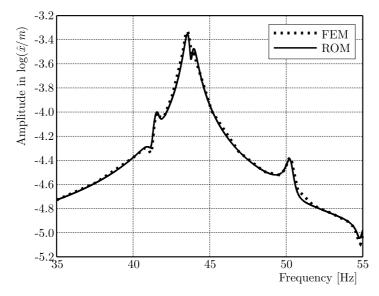
Fig. 5. Upper and lower limit of the FRF compared with a random mistuning for: (a) the first mode with $EO = 1$ and (b) the second and third mode with $EO = 3$

In all studies with the random mistuning, the upper limit fits well. In Fig. 6, a comparison of three sensitivity analyses with different numbers of terms of the Taylor series are given. The amplitudes are very close together but the behavior of the FRF is more detailed than with more terms. Calculating 1000 MCS, the PDF of all amplitudes can be compared with the PDF of the sensitivity analysis. The function of the PDF of the Gaussian distribution is given by

$$p(x) = \frac{1}{\sigma\sqrt{2\pi}} \exp\left[-\frac{1}{2}\left(\frac{x-\mu}{\sigma}\right)^2\right] \tag{3.13}$$

with σ derived from Eq. (3.8) and $\mu = u_0$ as the amplitude of the nominal system. In Figs. 7a and 7b, the probability distributions of the MCS and the Gaussian distrubtion of the sensitivity analysis using Eq. (3.13) are shown.
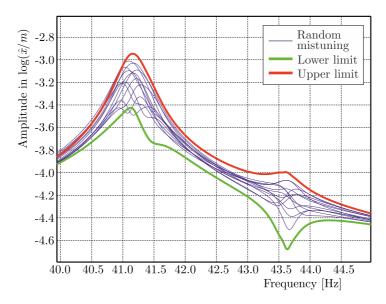

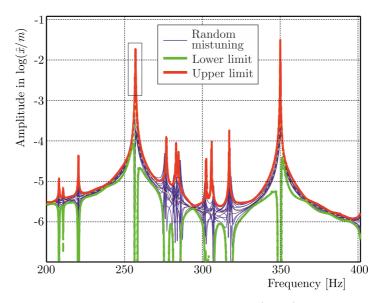Fig. 6. Comparison of different numbers of terms of the Taylor series (without MCS)

Fig. 7. (a) Comparison between 1000 Monte-Carlo simulations (MCS) and the sensitivity analysis (SA) with σ calculated at the first eigenfrequency at $41.15\,\mathrm{Hz}$ for $EO = 1$; (b) comparison between 1000 MCS and the PDF with σ calculated at the third eigenfrequency at $372.33\,\mathrm{Hz}$ for $EO = 4$

4. Case study: intentional mistuning

The second model has 30 blades which have an off-axis angle. The first mode is the one of interest. To show the generality of the reduction method, an intentional mistuning is introduced. This case study underlines the possibilities of such a method. A comparison between the reduced order model and the Finite-Element model is given in Hohl *et al.* (2011). With the sensitivity analysis a lot of parameter studies are feasible without consulting the calculating time. One of the most important ways to handle the increase of the amplitude is to use two different types of blades. For this purpose, an alternative pattern is used called AB mistuning. The benefits of this method are shown in Castanier and Pierre (2002), Han and Mignolet (2008), Mignolet *et al.* (2000) and Tatzko *et al.* (2013). An optimal intentional mistuning pattern is found for the frequency response including an additional random mistuning. In this way, costly statistics are used requiring a lot of computation time. With the sensitivity analysis shown here, the intentional mistuning can be classified as a simple method. To calculate the maximum amplitude of the pattern, the upper limit has to be calculated just once. This method is not restricted to just two different blade types or a geometric deviation.

The second blade is slightly thicker at its platform region, see Fig. 9. Therefore, it is necessary to rebuild the finite element mesh. Assuming that the contact nodes are at the same locations like the nodes of the disk, both types of blades are reduced using the Craig-Bampton with the same master nodes, as it is described in Eq. (2.17). With the same mesh at the contact nodes, the waves are the same for all blades. Only the reduced stiffness matrix of the blades is changed to

$$
[\operatorname{diag}(\widetilde{\mathbf{K}}_{b,ss})] = \begin{bmatrix} \delta_1 \widetilde{\mathbf{K}}_{b,ss}^{\mathrm{A}} & \mathbf{0} & \cdots & \mathbf{0} \\ \mathbf{0} & \delta_2 \widetilde{\mathbf{K}}_{b,ss}^{\mathrm{B}} & \cdots & \mathbf{0} \\ \vdots & \vdots & \ddots & \vdots \\ \mathbf{0} & \mathbf{0} & \cdots & \delta_N \widetilde{\mathbf{K}}_{b,ss}^{\mathrm{B}} \end{bmatrix} \tag{4.1}
$$

So, it is very simple to realize the intentional mistuning with geometric differences. The introduced sensitivity analysis is a suitable approach to estimate different patterns of the intentional mistuning using as many different blade types as required. The frequency response function
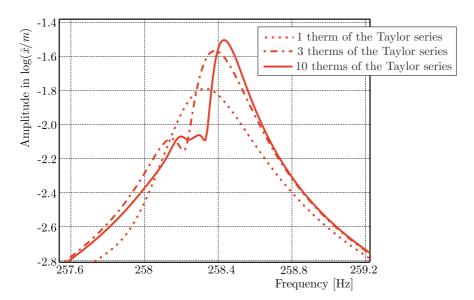
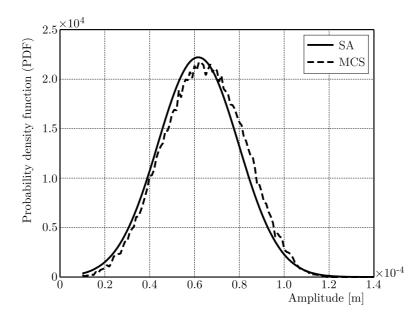Fig. 8. FEM of the second model blisk

Fig. 9. Two different blade types, including intentional mistuning

has to be calculated only once to have a good estimation for the pattern. In this paper, three different patterns are evaluated. The first version is an AB mistuning, where the blades are set in alternation. In the second version, three blades of the same type are collected and sorted alternately. In the third version, all blades of type A are arranged in a row, followed by all blades of type B arranged in a row (see Fig. 10).

These patterns are examples to show the benefits of the introduced methods. The results are unique for every blade and disk geometry and have to be reproduced for each example.

Regarding the vibration amplitude without aerodynamical coupling, the tuned system with only one blade type has the smallest amplitude. Due to areodynamical coupling, the intentional mistuning due to flutter or friction damping can be very useful. Nevertheless, the influence of the inevitable random mistuning has to be taken into account. With respect to the standard deviation of random mistuning, the three versions show small differences. With a very small standard deviation between 10^{-8} and 10^{-6}, version 3 is the best one. With a standard deviation higher than 10^{-5}, version 3 is the worst one. The chosen engine order is 2.
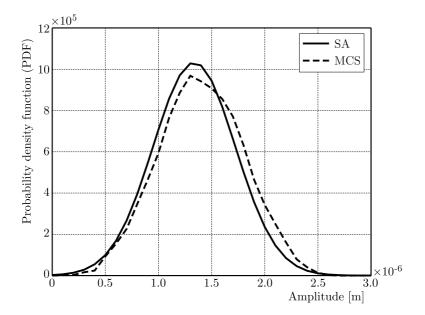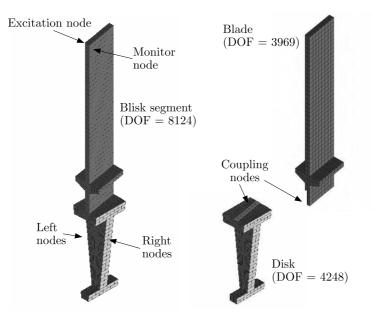
Fig. 10. Three patterns of the two blade types

Fig. 11. Maximum amplitude of the three patterns with respect to different standard deviations of the blades at $EO = 2$

Figure 12 shows the normalized amplitude with different engine orders with a standard deviation of 10^{-6}. Versions 1 and 2 are the most sensitive patterns at the first engine order.

5. Conclusions

In this paper, a new analytical method has been introduced to estimate the maximum amplitude of a mistuned bladed disk. Its benefits are proved by a simple model with characteristic dynamic behavior. After a short introduction of the model, the used reduction method has been presented. Therewith, the frequency response function has been calculated in a minimum of time and with good accuracy. Using the sensitivity analysis, the maximum amplitude for a given interval has been estimated. For this purpose, the force response function and the maximum amplitude have
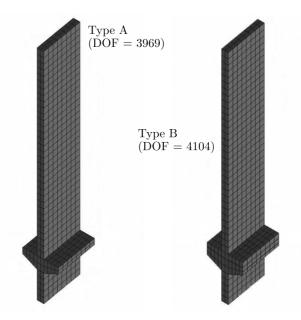
Fig. 12. Normalized amplitude with respect to the EO with a standard deviation of 10^{-6}

to be calculated only once. This saves a significant amount of time for optimization tools or parameter variations. Intentional AB mistuning has been presented as a possible application. Two types of blades have been used to analyze different patterns. The sensitivity analysis is proved to be a good tool for estimating intentional mistuning as well.

References

1. BECK J.A., BROWN J.M., CROSS C.J., SLATER J.C., 2012, Probabilistic mistuning assessment using nominal and geometry based mistuning methods, *Proceedings of ASME TURBO EXPO*

2. BHARTIYA Y., SINHA A., 2011, Reduced order model of a bladed rotor with geometric nistuning: comparison between modified modal domain analysis and frequency mistuning approach, *Proceedings of ASME TURBO EXPO*

3. BLADH R., CASTANIER M.P., PIERRE C., 2001a, Component-mode-based reduced order modeling techniques for mistuned bladed disks – part 1: Theoretical models, *Journal of Engineering for Gas Turbines and Power*, **123**, 89-98

4. BLADH R., CASTANIER M.P., PIERRE C., 2001b, Component-mode-based reduced order modeling techniques for mistuned bladed disks – part 2: Application, *Journal of Engineering for Gas Turbines and Power*, **123**, 100-108

5. BLADH R., PIERRE C., CASTANIER M.P., KRUSE M.J., 2001, Dynamic response predictions for a mistuned industrial turbomachinery rotor using reduced-order modeling, *Journal of Engineering for Gas Turbines and Power*, **123**, 100-108

6. CASTANIER M.P., PIERRE C., 2002, Using intentional mistuning in the design of turbomachinery rotors, *AIAA Journal*, **40**, 10, 2077-2086

7. CASTANIER M.P., PIERRE C., 2006, Modeling and analysis of mistuned bladed disk vibration: Status and emerging directions, *Journal of Propulsion and Power*, **22**, 2, 384-396

8. ČERMELJ P., PLUYMERS B., DONDERS S., DESMET W., BOLTEŽAR M., 2008, Basis functions and their sensitivity in the wave-based substructuring approach, *Proceedings of ISMA*

9. CRAIG R.R., 2000, Coupling of substructures for dynaimc analyses: An overview, *American Institute of Aeronautics and Astronautics*, **1573**, 3-14

10. CRAIG R.R., BAMPTON M.C.C., 1968, Coupling of substructures for dynamic analyses, *American Institute of Aeronautics and Astronautics*, **6**, 1313-1317

11. FEINER D.M., GRIFFIN J.H., 2002, A fundamental model of mistuning for a single family of modes, *Journal of Turbomachinery*, **124**, 597-605

12. FEINER D.M., GRIFFIN J.H., 2004a, Mistuning identification of bladed disks using a fundamental mistuning model – part I: Theory, *Journal of Turbomachinery*, **126**, 150-158

13. FEINER D.M., GRIFFIN J.H., 2004b, Mistuning identification of bladed disks using a fundamental mistuning model – part II: Application, *Journal of Turbomachinery*, **126**, 159-165

14. GRIFFIN J.H., HOOSAC T., 1984, Model development and statistical investigation of turbine blade mistuning, *Journal of Vibration, Acoustics, Stress, and Reliability*, **106**, 204-210

15. HAN Y., MIGNOLET M.P., 2008, Optimization of intentional mistuning patterns for the mitigation of the effects of random mistuning, *Proceedings of ASME TURBO EXPO*

16. HOHL A., KRIEGESMANN B., WALLASCHEK J., PANNING L., 2011, The influence of blade properties on the forced response of mistuned bladed disks, *Proceedings of ASME TURBO EXPO*

17. MIGNOLET M.P., HU W., 1997, Direct prediction of the effects of mistuning on the forced response of bladed disks, *International Gas Turbine and Aeroengine Congress and Exhibition*

18. MIGNOLET M.P., HU W., JADIC I., 2000, On the forced response of harmonically and partially mistuned bladed disks. part I: Harmonic mistuning, *International Journal of Rotating Machinery*, **6**, 1, 29-41

19. MIGNOLET M.P., RIVAS-GUERRA A., LABORDE B., 1999, Towards a comprehensive direct prediction strategy of the effects of mistuning on the forced response of turbomachinery blades, *Aircraft Engineering and Aerospace Technology*, **71**, 5, 462-469

20. MOYROUD F., FRANSSON T., JACQUET-RICHARDET G., 2002, A comparison of two finite element reduction techniques for mistuned bladed disks, *Journal of Engineering for Gas Turbines and Power*, **124**, 942-952

21. PETROV E.P., 2011, Reduction of forced response levels for bladed disks by mistuning: Overview of the phenomenon, *Journal of Engineering for Gas Turbines and Power*, **133**, 072501-1-072501-10

22. SEXTRO W., PANNING L., GOETTING F., POPP K., 2002, Fast calculation of the statistics of the forced response of mistuning bladed disk assemblies with friction contracts, *Proceedings of ASME TURBO EXPO*

23. SHUAI W., JIANYAO Y., 2010, Mistuning identification for integrally bladed disks based on the SNM technique, *Proceedings of ASME TURBO EXPO*

24. SIEWERT C., STÜER H., 2010, Forced response analysis of mistuned turbine bladings, *Proceedings of ASME TURBO EXPO*

25. SINHA A., 1986, Calculating the statistics of forced response of a mistuned bladed disk assembly, *AIAA Journal*, **24**, 11

26. SINHA A., 2009, Reduced-order model of a bladed rotor with geometric mistuning, *Journal of Turbomachinery*, **131**, 031007-1-031007-7

27. SINHA A., CHEN S., 1989, A higher order technique to compute the statistics of forced response of a mistuned bladed disk assembly, *Journal of Sound and Vibration*, **130**, 2, 207-221

28. TATZKO S., VON SCHEIDT L.P., WALLASCHEK J., KAYSER A., WALZ G., 2013, Investigation of alternate mistuned turbine blades non-linear coupled by underplatform gampers, *Proceedings of ASME TURBO EXPO*

29. THOMAS D.L., 1979, Dynamics of rotationally periodic structures, *International Journal for Numerical Methods in Engineering*, **14**, 81-102

30. WHITEHEAD D.S., 1966, Effect of mistuning on the vibration of turbomachine blades induced by wakes, *Journal Mechanical Engineering Science*, **8**, 1, 15-21

31. YANG M.-T., GRIFFIN J.H., 2001, A reduced-order model of mistuning using a subset of nominal system modes, *Journal of Engineering for Gas Turbines and Power*, **123**, 893-900